

## CHAPTER 229

### The Kinematics of Wave Induced Flows Around Near-Bed Pipelines

T.Bruce<sup>1</sup>, W.J.Easson<sup>2</sup>

#### ABSTRACT

Particle Image Velocimetry (PIV) has been applied successfully to give quantitative, full field measurements of instantaneous velocity fields for oscillatory flows past a model of a pipeline above a plane bed. The application of PIV to this problem is discussed, and results for the case of  $KC = 20$  with gap ratios 1.0 and 0.1 are presented in the form of velocity vector maps, and contour plots of vorticity distribution.

#### INTRODUCTION

There is extensive coverage in the literature of research into the fluid loadings experienced by cylindrical structures in a wide variety of flow regimes [eg. Sarpkaya, Isaacson, 1980]. Many studies have focussed on the cyclic variation of drag and lift forces on a horizontal cylinder exposed to wave action. Some of these studies have been extended to investigate the effect of the proximity of a plane bed on cylinder loadings.

Recently, qualitative flow visualisation studies have improved the understanding of loading cycles through wave periods. Williamson [1985] performed simultaneous visualisations and force measurements for a cylinder being oscillated at  $KC$  numbers up to 60, and was able to relate the form of the loading-time curve to the vortex shedding process in a number of distinct shedding regimes. Sumer et al [1991] have extended this work to investigate the influence of a plane boundary close to the cylinder.

The objective of the work reported here was to obtain quantitative, full-field measurements of the kinematics of oscillatory flows past a cylinder near a plane boundary. These flows are unsteady, so building up a quantitative map of the kinematics using a single point measurement technique would be impossible. Attention must therefore be turned to techniques which can measure velocities over

---

<sup>1</sup>Research Associate, Dept. of Mechanical Engineering, The University of Edinburgh, King's Buildings, Edinburgh, EH9 3JL, Scotland. (T.Bruce@ed.ac.uk)

<sup>2</sup>Lecturer, Dept. Mech. Eng (will@mech.ed.ac.uk)

a complete, two-dimensional measurement zone. Established methods such as streak photography which readily give qualitative flow visualisations can be made to yield quantitative data, but the analysis can be laborious and the errors involved are in general large. A technique which suffers none of the above drawback is Particle Image Velocimetry (PIV), and it is this technique's application to oscillatory flows past near-bed cylinders which is described here.

The numerical modelling of unsteady flows past cylinders is becoming increasingly successful. The discrete vortex model has been applied to the flow past a cylinder above a plane boundary [Penoyre and Stansby, 1988] with promising results. However, in order to assess the validity of these models, accurate, full-field quantitative data for the flow kinematics is required. Also, quantitative data of this kind may find use in the modelling of sediment transport and the scour process in the vicinity of a seabed pipeline.

## METHOD

PIV is a relatively new technique which gives a quantitative map of instantaneous flow velocities over a large area. Additionally, the velocities obtained are of high accuracy and high resolution. The basis of PIV is to stroboscopically illuminate a two-dimensional plane through the flow, which has been *seeded* with tiny reflective particles which are assumed to follow the flow accurately. The illuminated plane is then photographed, the shutter being held open long enough to record at least two illuminations. Thus each seeding particle gives rise to at least two particle images. The local flow can then be determined from the separation of these images. A fully automated system is used to *interrogate* the photograph over an array of points to build up a flow velocity map. A detailed description and appraisal of PIV is presented elsewhere in the proceeding of this conference [Greated et al, 1992].

A purpose-built facility has been constructed for these studies, consisting of a rectangular 6m by 1m tank with a water depth of 0.5m, above which runs a computer controlled trolley (figure 1). This trolley tows objects through initially stationary water, and may be programmed to execute complex motion sequences. For the experiments reported here, a horizontal test cylinder (of diameter 50mm) and a false bed were rigidly attached to the trolley and were towed through the tank to give a sinusoidal motion. In general, the flow kinematics resulting from moving an object sinusoidally through initially stationary fluid are identical to those generated by a sinusoidal fluid flow past a fixed object [Garrison, 1980]. However, in the case being studied, it was important that the influence of the bed on the kinematics was correctly included in the tests: In order that the finite length of the false bed did not affect the flows observed, the false bed was more than twice the length of the largest amplitude oscillations.

A two-dimensional plane in the flow is illuminated stroboscopically through the glass bottom of the tank by a 15W Argon Ion continuous wave laser and a *scanning beam* system [Greated et al, 1992, Gray et al, 1991]. The flow is seeded

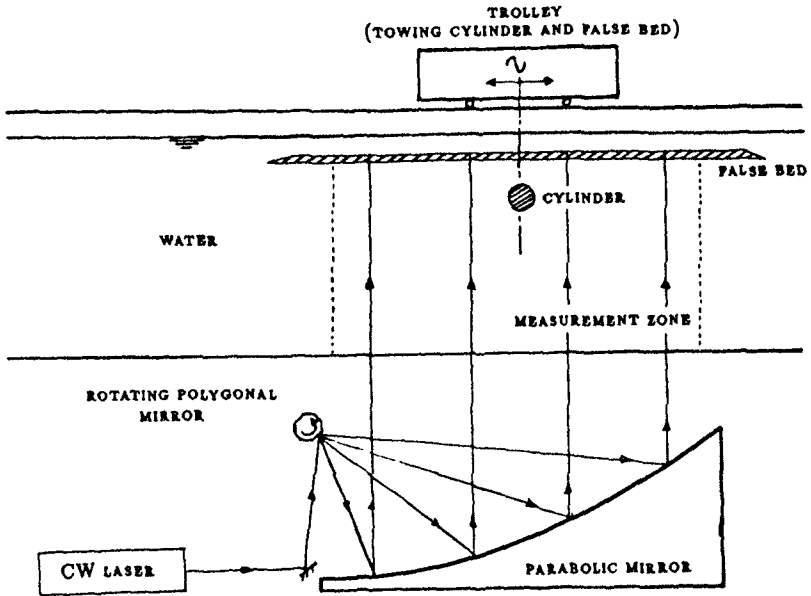


Figure 1: Experimental facility

with conifer pollen and photographed using a Hasselblad *EL/M* medium (55mm) format camera. For these experiments, the camera was triggered electronically from the trolley control system, so that a precise phase of the flow could be selected and captured. Additionally, the camera was panned across the measurement field as the photograph was taken. The reason that it was necessary to pan the camera is as follows:

PIV in its basic form gets velocity information from the separations of double particle images on a photograph. In general there is no way to tell which image is the first, and thus there exists an inherent ambiguity in the sense of the velocity measurement obtained at any given point. In many, indeed most cases, this does not cause a problem; eg in the case of a breaking wave, it is known *a priori* all the motion is in one  $180^\circ$  arc. However, in this application, there are both forward and reverse flows present. Also, PIV in its basic form cannot positively measure a region of zero flow velocity — it relies on measuring the separation of correlated particle images, and if the first and second images overlap, then no correlated separation will be visible and thus no velocity measurable.

Panning the camera as the photograph is taken solves both these problems: As it is being panned, the camera sees the whole flow field as if a large *shift*

velocity had been imposed on the true flow field. The velocities recorded will have this large offset superposed on the true flow. If this *shift* velocity is made sufficiently large, the first particle image will always be to the same side of the second, and particle images which would have been coincident in areas of very low or zero flow velocity are now separated. The shift can be subsequently subtracted from the measured field to give the true flow field. (This *image shifting* technique is analogous to *frequency shifting* in LDA).

## EXPERIMENTAL PARAMETERS

The formation of vortices at the pipeline, and the subsequent motion of these vortices (particularly when they are *swept back* over the pipeline) strongly affect the drag and lift forces on the pipeline. Naturally, the pattern of vortex formation and movement varies a great deal for different flow regimes. The structure of these flows past a smooth pipeline is governed by three dimensionless parameters:

The Keulegan Carpenter number (KC) is defined as

$$KC = \frac{U_m \tau}{D}$$

where  $U_m$  is the magnitude of the maximum velocity of the oscillatory flow,  $\tau$  is the period of the oscillation and  $D$  is the characteristic dimension of the flow; here, the cylinder diameter. Thus the larger KC, the larger the motion of *fluid particles* relative to the size of the cylinder.

The second important parameter is the *gap ratio*,  $e/D$ .

$$e/D = \frac{\text{size of gap between cylinder and bed}}{\text{cylinder diameter}}$$

Finally, the Reynolds number ( $R_e$ )

$$R_e = \frac{U_m D}{\nu}$$

where  $\nu$  is the kinematic viscosity.

The structure of the flow is strongly affected by the combination of KC and  $e/D$ . However, the dependence on  $R_e$  is only weak — all the flows studied here are sub-critical, and the form of the flow is largely independent of  $R_e$  within the sub-critical range of  $R_e$ .

Williamson [1985] studied oscillatory flows past a cylinder in free stream (ie, without a plane boundary) and identified distinct ranges of KC values over which a particular pattern of vortex formation and motion was observed. Sumer et al [1991] reviewed the flow patterns in these regimes for various values of the gap

ratio  $e/D$ . He presents visualisations and loading measurements for  $KC = 4, 10, 20, 30$  and  $e/D$  over the range from 0 to 3.5.

This paper presents results of the first experiments in this study. As such, the work of Sumer et al was considered an excellent starting point. The cases of  $KC = 20$  with  $e/D = 1.0$  and  $e/D = 0.1$  were the first to be studied, and it is these tests that are reported here.

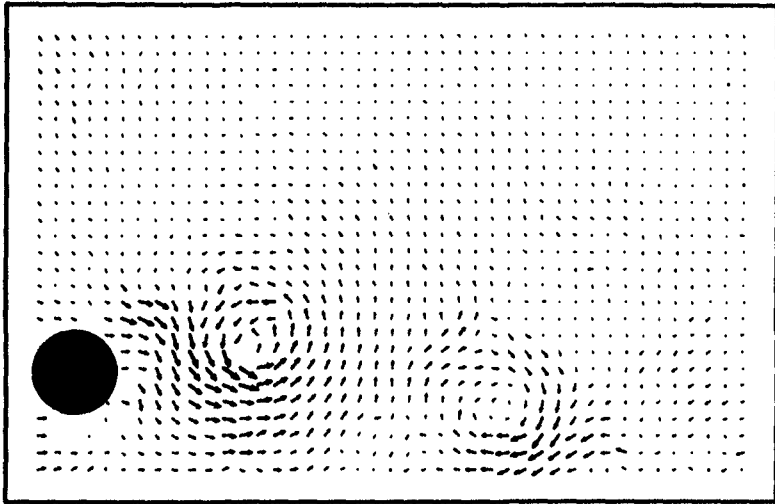


Figure 2: Velocity vectors,  $KC = 20$ ,  $e/D = 1.0$ , phase =  $0^\circ$

## RESULTS

Once the process of obtaining good PIV images has been established for a given application, it is possible to obtain large quantities of data in a short time. Here, there are a large number of flow regimes of interest, each characterised by  $KC$  and  $e/D$  parameters. For each regime, there are a number of interesting events (eg vortex separation) which should be recorded. The results presented here have been chosen to be illustrative of the sort of data obtained. The data is presented in two forms: as velocity vector maps, and as contour plots of the vorticity distribution.

Figure 2 is an example of a velocity vector map. Each of the vectors corresponds to one analysed point on the PIV photograph, so the flow has been measured at around 1000 points from the PIV photograph. No interpolation has been carried out on the data. The map shows the measured flow at the end of one

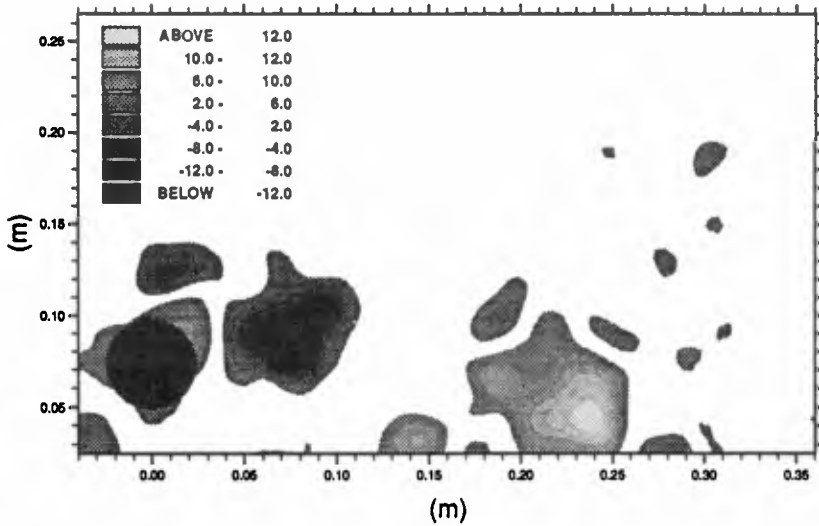


Figure 3: Vorticity,  $KC = 20$ ,  $e/D = 1.0$ , phase =  $0^\circ$

half-cycle for the case  $KC = 20$ ,  $e/D = 1.0$ . The model pipe is instantaneously at rest having moved from right to left over the previous half cycle.

Some interesting features of the flow stand out immediately. There are two vortices clearly visible. The vortex just to the right of the pipe has just been shed. Its rotation is counter-clockwise, so before it was shed, it developed on the side of the pipe adjacent to the wall. In addition to this *wall-side* vortex, there is a second vortex rotating clockwise near the bed whose origin is not clear from this map alone.

An alternative way to present the data is in the form of a map of vorticity distribution. Figure 3 shows the vorticity distribution derived from the same data as shown in figure 2.

The vorticity ( $\Omega$ ) at a point  $(x,y)$  in the field was calculated from

$$\Omega(x, y) = \frac{v_x(x, y + \delta y) - v_x(x, y - \delta y)}{2\delta y} - \frac{v_y(x + \delta x, y) - v_y(x - \delta x, y)}{2\delta x}$$

where the  $v_x(x, y)$  and  $v_y(x, y)$  are the x and y components of the measured velocity at  $(x,y)$ , and  $\delta x$ ,  $\delta y$  is the separation in space between neighbouring ve-

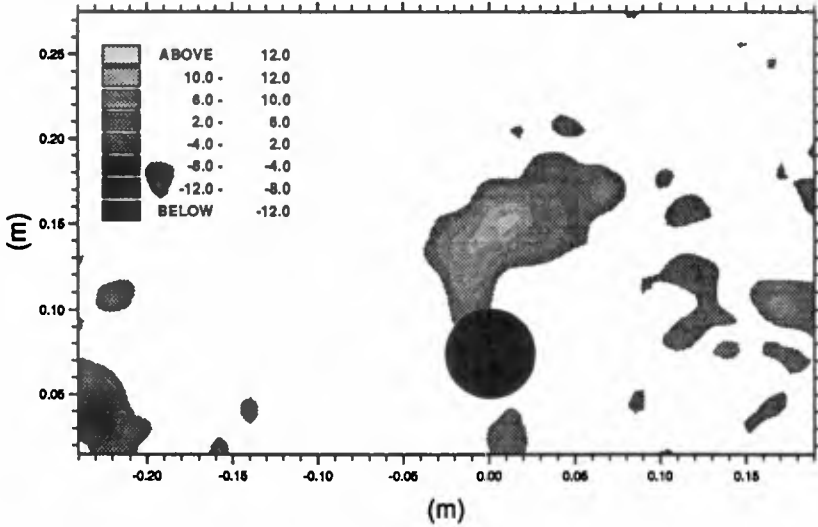


Figure 4: Vorticity,  $KC = 20$ ,  $e/D = 1.0$ , phase =  $270^\circ$

locity points. Such numerical differentiation is very susceptible to errors, but the smoothness of the resulting distribution indicates that these errors are acceptably small.

The white background indicates areas where there is little or no vorticity (or rotation) in the flow. The contoured areas leading to a light centre indicate positive vorticity (clockwise rotation), and the areas leading to a dark centre indicate negative (counter-clockwise rotation). In this case, the structure of the flow is clearly visible on both vector and vorticity maps. However, when there is an area of weak vorticity, this structure often only becomes clearly visible when the vorticity is calculated.

Figure 4 shows the vorticity distribution a quarter cycle ( $90^\circ$ ) before that shown in figure 3, and helps clarify the origin of the large region of positive vorticity visible near the bed in the middle of the previous plots. Here, the pipe is moving from right to left at its maximum velocity of  $200\text{mms}^{-1}$ . It shows clearly a positive vortex being washed over the pipe. It is this vortex which subsequently appears as the rightmost vortex in figure 3. This vortex was the wall-side vortex shed during the previous half-cycle.

When the gap ratio  $e/D$  is reduced from 1.0 to 0.1, the structure of the flow is quite different. Only one vortex (the wall-side vortex) of any size develops

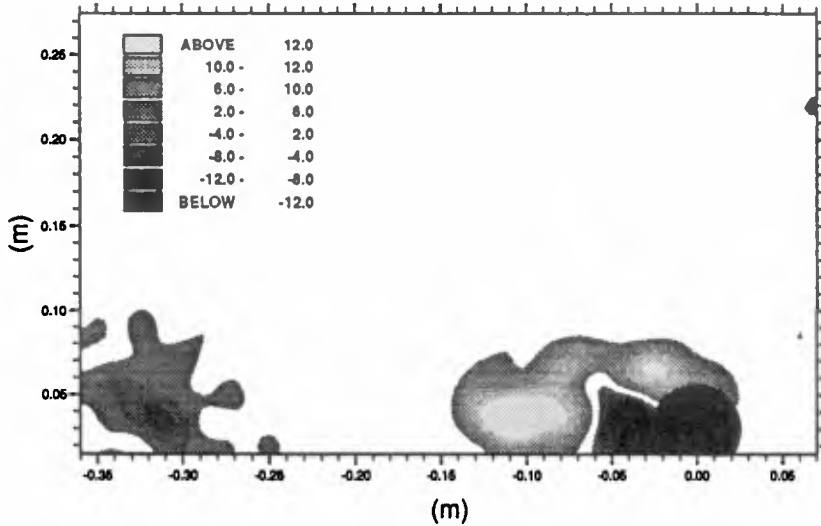


Figure 5: Vorticity,  $KC = 20$ ,  $e/D = 0.1$ , phase =  $165^\circ$

during a half-cycle, and this happens quite near the end of the half-cycle. As the pipe comes to rest and begins to move back on the next half cycle, this vortex is promptly washed back across the pipe. Figure 5 shows the flow as measured at a phase of  $165^\circ$ , just before the end of the left to right half cycle. The wall-side vortex is quite well developed and clearly visible. Also visible is a small area of negative vorticity, lower left of the map. This area is the remnant of the wall-side vortex from the previous half-cycle which was washed over the pipe during the current half-cycle.

## CONCLUDING REMARKS

PIV has been successfully applied to a model of a pipeline above a plane seabed. The quality of the first velocity maps and vorticity contour maps is most encouraging, and detailed comparison with numerically modelled flows should be possible.

In the immediate future, this study will be extended to survey a number of other  $KC$  and  $e/D$  combinations which are representative of the various different flow regimes. It is hoped to place particular emphasis on those flow regimes most relevant to the real coastal environment.

Following the studies of the plane bed, it is intended to move on to investigate

the new kinematics in the case of a scoured bed below the pipeline, and also the case of interaction between cylindrical structures.

## REFERENCES

- Garrison, C.J. (1980).  
*A Review of Drag and Inertia Forces on Circular Cylinders.*  
Proc. 12th Offshore Technology Conference, pp 205-218.
- Gray, C., Greated, C.A., McCluskey, D.R. & Easson, W.J. (1991).  
*An Analysis of the Scanning Beam PIV Illumination System.*  
Journal of Physics (Measurement Science and Technology), 2, pp717-724.
- Penoyre, R.B.S. & Stansby, P.K. (1988).  
*A Computer Program for Simulating Flow Past a Cylinder Above a Plane Boundary.*  
Report of the Simon Engineering Laboratory, University of Manchester.
- Sarpkaya, T. & Isaacson, M. (1981).  
*Mechanics of Wave Forces on Offshore Structures.*  
Van Nostrand Reinhold.
- Skyner, D.J., Gray, C. & Greated, C.A. (1990).  
*A Comparison of Time-Stepping Numerical Predictions with Whole-Field Flow Measurement in Breaking Waves.*  
Water Wave Kinematics, pp491-508, Kluwer Academic Publishers.
- Sumer, B.M., Jenson, B.L. & Fredsøe, J. (1991).  
*Effect of a Plane Boundary on Oscillatory Flow Around a Circular Cylinder.*  
Journal of Fluid Mechanics, 225, pp271-300.
- Williamson, C.H.K. (1985).  
*Sinusoidal Flow Relative to Circular Cylinders.*  
Journal of Fluid Mechanics, 155, pp141-174.